

# Evaluation of Interpolation Methods for Motion Compensated Tomographic Reconstruction for Cardiac Angiographic C-arm Data

Kerstin Müller, Yefeng Zheng, Günter Lauritsch, Christopher Rohkohl, Chris Schwemmer, Andreas K. Maier, Rebecca Fahrig and Joachim Hornegger

**Abstract**—Anatomical and functional information about the cardiac chambers is a key component of future developments in the field of interventional cardiology. With the technology of C-arm CT it is possible to reconstruct intraprocedural 3-D images from angiographic projection data. Some approaches attempt to add the temporal dimension (4-D) by electrocardiogram (ECG)-gating in order to distinguish physical states of the heart. However, for the left heart ventricle scanned during one single C-arm sweep, this approach leads to insufficient projection data and thus to a degraded image reconstruction quality.

In this paper, we evaluate the influence of different interpolation methods for a motion compensated reconstruction approach for the left heart ventricle based on a recently presented 3-D dynamic surface model. The surface model results in a sparse motion vector field (MVF) defined at control points. However, to perform a motion compensated reconstruction a dense MVF is required. The dense MVF can be determined by different interpolation methods. In this paper, we evaluate thin-plate splines (TPS), the Shepard's method, simple averaging, and a smoothed weighting function as interpolation functions. The 2-D overlap of the forward projected motion compensated reconstructed ventricle and the segmented 2-D ventricle blood pool is quantitatively measured with the Dice similarity coefficient and the mean deviation between extracted ventricle contours. Preliminary results on heart ventricle phantom data, as well as on clinical human data show the best results with the TPS interpolation.

## I. INTRODUCTION

### A. Purpose of this Work

There is increasing interest in three-dimensional imaging of dynamic cardiac ventricular shapes, e.g. left ventricle (LV) motion, for quantitative evaluation of cardiac function such as ejection fraction measurements and wall motion analysis. Typically these parameters are estimated based on 2-D projections from two or less views [1]. The 2-D approach lacks information about the 3-D shape of the LV. A 3-D reconstruction with projection data from a short-scan permits the physician to assess the LV in all spatial dimensions. Due to the long acquisition time (a few seconds) of the C-arm,

the dynamics of the ventricle need to be taken into account. A standard cone-beam reconstruction (FDK) [2] averages over all heart phases and has no temporal resolution. Therefore, a motion compensated tomographic reconstruction for the heart ventricle should be developed. An accurate estimate of the motion would also provide a direct analysis of the temporal characteristics of the ventricle.

### B. State-of-the-Art

Different approaches for recovering ventricular shapes from angiographic data using biplanar angiographic systems can be found in the literature [1], [3]. These systems can acquire two orthogonal projection images simultaneously. However, such a biplanar system is not accessible to all cardiologists.

Another approach records an ECG signal during acquisition and a relative heart phase is assigned to each projection. Commonly, the heart phases are then denoted as a percentage between two successive R-peaks. In order to improve temporal resolution, the reconstruction is performed with the subset of the projections that lie inside a certain ECG window centered at the favored heart phase [4]. As an example, for a 5 s acquisition time and 60 bpm five intervals contribute to one heart phase. The ECG-gated approach works well for the sparse and high contrasted structure of the coronaries [5]–[7]. However, for the heart chambers an insufficient number of projections are acquired in a single scan. Consequently, multiple sweeps of the C-arm have to be performed in order to acquire enough projections for each heart phase [8], [9]. The longer imaging time results in a higher contrast burden and radiation dose for the patient.

In this paper, we perform a motion compensated tomographic reconstruction with projection data from one single C-arm sweep. As a first step, a dynamic surface model of the LV is generated to extract a sparse MVF [10]. The LV surface model is reconstructed from a set of ECG-gated 2-D X-ray projections such that the forward projection of the reconstructed LV model matches the 2-D blood pool segmentation of the ventricle. In the second step, a motion compensated tomographic reconstruction is performed. This requires a dense MVF [11]. Thus, the sparse motion field on the surface has to be interpolated. In order to generate a dense MVF from scattered data several interpolation methods can be applied

K. Müller, C. Schwemmer and J. Hornegger are with the Pattern Recognition Lab, Department of Computer Science and the Erlangen Graduate School in Advanced Optical Technologies (SAOT), Friedrich-Alexander-Universität Erlangen-Nürnberg, Erlangen, Germany. Email:kerstin.mueller@cs.fau.de. G. Lauritsch, C. Rohkohl and A. K. Maier are with the Siemens AG, Healthcare Sector, Forchheim, Germany. Y. Zheng is with Image Analytics and Informatics, Siemens Corporate Research, Princeton, NJ, USA. R. Fahrig is with the Department of Radiology, Stanford University, Stanford, CA, USA.

[12]. For computed tomography (CT) image reconstruction, different interpolation methods for cardiac motion were investigated by Forthmann et al [13]. However, the main focus of the reconstruction was on the sharpness of the coronaries. Furthermore, C-arm projection data displays different contrast conditions and suffers from a lower temporal resolution than a conventional CT scanner. Therefore, it is not evident that the same interpolation methods yield the same results.

### C. Outline

In this paper, we investigate different interpolation methods: a thin-plate spline (TPS) interpolation [14], [15], the Shepard's method [16], a simple averaging, and a weighting function based interpolation method. The interpolation methods were evaluated by comparing the image results of the motion compensated tomographic reconstructions with the gold standard of the segmented original projection data.

## II. SURFACE BASED MOTION COMPENSATED RECONSTRUCTION

### A. Surface Model

The basis of the motion compensated reconstruction is the dynamic 3-D surface of the ventricle with its control points  $\mathbf{p}_i(\phi_k) \in \mathbb{R}^3$ , with  $i = 1, \dots, N$  where  $N$  is the number of control points for each heart phase  $\phi_k$  [10]. For reconstruction a reference heart phase  $\phi_0$  is selected. Displacement vectors  $\mathbf{d}_i(\phi_k) \in \mathbb{R}^3$  between the control points in the reference heart phase  $\phi_0$  and the current heart phase  $\phi_k$  can then be computed.

### B. Interpolation Methods

In order to perform a motion compensated tomographic reconstruction, a dense MVF needs to be generated from the sparse MVF. Therefore, different interpolation methods were evaluated.

1) *Thin-Plate Splines (TPS)*: The deformation of the control points over time can be represented by a TPS transformation. The TPS approach assumes that the bending and stretching behavior of the left ventricle is similar to the bending of a thin plate. TPS have already been applied to estimate cardiac vascular motion of CT data [17] and ventricular motion of MRI data [18].

The TPS coordinate transformation with its displacements for an arbitrary point  $\mathbf{x} \in \mathbb{R}^3$  is given as:

$$\mathbf{d}(\mathbf{x}, \phi_k) = \sum_{i=1}^N \mathbf{G}(\mathbf{x} - \mathbf{p}_i(\phi_k)) c_i(\phi_k) + \mathbf{A}(\phi_k) \mathbf{x} + \mathbf{b}(\phi_k), \quad (1)$$

where the spline coefficients  $c_i(\phi_k) \in \mathbb{R}$  of the TPS are determined by the control points  $\mathbf{p}_i(\phi_k) \in \mathbb{R}^3$  and the displacements  $\mathbf{d}_i(\phi_k) \in \mathbb{R}^3$  of the control points.  $\mathbf{A}(\phi_k) \in \mathbb{R}^{3 \times 3}$ ,  $\mathbf{b}(\phi_k) \in \mathbb{R}^3$  specify an additional affine transformation to which the spline reduces farther away from the control points. The transformation's kernel matrix  $\mathbf{G}(\mathbf{x}) \in \mathbb{R}^{3 \times 3}$  of a point  $\mathbf{x} \in \mathbb{R}^3$  for a 3-D TPS is given according to [15]:

$$\mathbf{G}(\mathbf{x}) = r(\mathbf{x}) \cdot \mathbf{I}, \quad (2)$$

$$r(\mathbf{x}) = \|\mathbf{x}\|_2 = \sqrt{x_1^2 + x_2^2 + x_3^2}, \quad (3)$$

where  $\mathbf{I} \in \mathbb{R}^{3 \times 3}$  is the identity matrix. In order to solve Equation 1 for each  $\phi_k$ , set  $\mathbf{d}(\mathbf{x}, \phi_k) = \mathbf{d}(\phi_k)$  for  $\mathbf{x} = \mathbf{p}_i(\phi_k)$ . Since Equation 1 is linear in  $c_i(\phi_k)$ ,  $\mathbf{A}(\phi_k)$ , and  $\mathbf{b}(\phi_k)$  it can be solved in a straightforward manner [15].

The resulting spline coefficients and affine parameters are inserted in Equation 1 in order to evaluate the spline at any arbitrary 3-D point. A motion vector can therefore be computed for every voxel in the reconstructed volume.

2) *Linear Interpolation*: All surface control points inside a radius  $R$  (here: 2 cm) around the point  $\mathbf{x}$  are determined and the resulting displacement vector  $\mathbf{d}(\mathbf{x}, \phi_k)$  is a weighted sum of the corresponding displacement vectors:

$$\mathbf{d}(\mathbf{x}, \phi_k) = \sum_{i=1}^N \mathbf{G}^*(\mathbf{x} - \mathbf{p}_i(\phi_k)) \mathbf{d}_i(\phi_k), \quad (4)$$

$$\mathbf{G}^*(\mathbf{x}) = f(\mathbf{x}) \cdot \mathbf{I}, \quad (5)$$

where  $f$  is a weighting function. Function  $f$  weights the displacement vectors according to the distance of the control point  $\mathbf{p}_i(\phi_k)$  to the point  $\mathbf{x}$ .

a) *Simple Averaging*: Here the resulting displacement vector  $\mathbf{d}(\mathbf{x}, \phi_k)$  is a simple average of the displacement vectors at the surrounding control points. Thus the function  $f$ , with  $M$  denoting the number of control points used is defined as:

$$f(\mathbf{x}) = \begin{cases} \frac{1}{M} & |\mathbf{x}| \leq R \\ 0 & \text{else} \end{cases} \quad (6)$$

b) *Weighting Function*: Here the function  $f$  is a cosine-based smoothing function:

$$f(\mathbf{x}) = \begin{cases} \frac{1}{N} (1 + \cos(\frac{\mathbf{x} \cdot \pi}{R})) & |\mathbf{x}| \leq R \\ 0 & \text{else,} \end{cases} \quad (7)$$

where  $N$  denotes a normalization constant such that  $\sum_{j=1}^M f(\mathbf{x}_j) = 1$ .

c) *Shepard's Method*: Here an inverse distance weighting is applied according to the distance from the considered point to the  $n$  closest control points [16]. The function  $f$  is therefore defined as:

$$f(\mathbf{x}) = \frac{\|\mathbf{x}\|_2^{-1}}{\sum_{j=1}^n \|\mathbf{x}_j\|_2^{-1}}. \quad (8)$$

We set  $n$  empirically to 30 in this paper.

### C. Cutting

In order to reduce the computational complexity we assume that the left ventricle is the central moving organ inside the scan field of view. Therefore, a dense MVF is computed inside the ventricle and within a neighborhood around the extracted surface of the first section of the ascending aorta and the ventricle. Hence, the considered set of points  $\mathcal{P}$  is given as:

$$\mathcal{P} = \{\mathbf{x} \mid \|\mathbf{x} - \mathbf{p}_x(\phi_k)\|_2 \leq l\}, \quad (9)$$

where  $\mathbf{p}_x(\phi_k)$  is the closest surface control point to the current point  $\mathbf{x}$ . The distance  $l$  was heuristically set to 2 cm.

### III. EXPERIMENTS

#### A. Phantom Data

The presented algorithm has been applied to a ventricle data set comparable to the XCAT phantom [19]. We simulated data using a clinical protocol with the following parameters: 395 projection images simulated equi-angularly over an angular range of  $200^\circ$  in 8 s with a size of  $620 \times 480$  pixels at an isotropic resolution of 0.62 mm/pixel ( $\approx 0.4$  mm in isocenter). The heartbeat was simulated with 75 bpm. The surface model consisted of 40 heart phases and 957 control points uniformly distributed over the left ventricle. The image reconstruction was performed on an image volume of  $(25.6 \text{ cm})^3$  distributed on a  $256^3$  voxel grid.

#### B. Clinical Data

The dataset was acquired on an Artis Zee C-arm system (Siemens AG, Healthcare Sector, Forchheim, Germany). It consists of 133 projection images acquired over an angular range of  $200^\circ$  in 5 s with a size of  $960 \times 960$  pixels at an isotropic resolution of 0.18 mm/pixel ( $\approx 0.12$  mm in isocenter). The patient had a heart rate of  $\approx 60$  bpm. The surface model consisted of 26 heart phases and 961 control points equally distributed over the first section of the ascending aorta and left ventricle. Image reconstruction was performed on an image volume of  $(14.1 \text{ cm})^3$  distributed on a  $256^3$  voxel grid.

#### C. Quantitative Evaluation

In order to compare the reconstruction quality of the motion compensated reconstruction algorithm, the maximum intensity forward projections (MIP) of the compensated LVs were generated. Binary mask images were created from the MIPs where a value equal to zero defines background and a non-zero value defines the ventricle shape. These binary images were compared to the segmented 2-D projections from which the original surface model was built. The overlap of the binarized image and the segmented 2-D projections was analyzed with the Dice similarity coefficient (DSC) [20]. The DSC is defined in the range of  $[0, 1]$ , where 0 means no overlap and 1 defines a perfect match between the two compared images. Since the motion compensated reconstruction improves the sharpness of the ventricle contour, the similarity of the contours of the projection images were evaluated with the mean deviation between the contours denoted by  $\epsilon$ , where a small  $\epsilon$  denotes a similar contour. The results were averaged over all heart phases.

### IV. RESULTS AND DISCUSSION

In Figure 1, an MVF of the human data set between the reference heart phase at end-diastole and the current heart phase at end-systole are illustrated for the TPS.

#### A. Phantom Data

In Table I the results for the phantom left ventricle are reported. The best results were obtained with the TPS interpolation method. The contour deviation ( $\epsilon$ ) improved by  $\approx 2$  pixel which corresponds to 1.24 mm compared to the standard FDK.

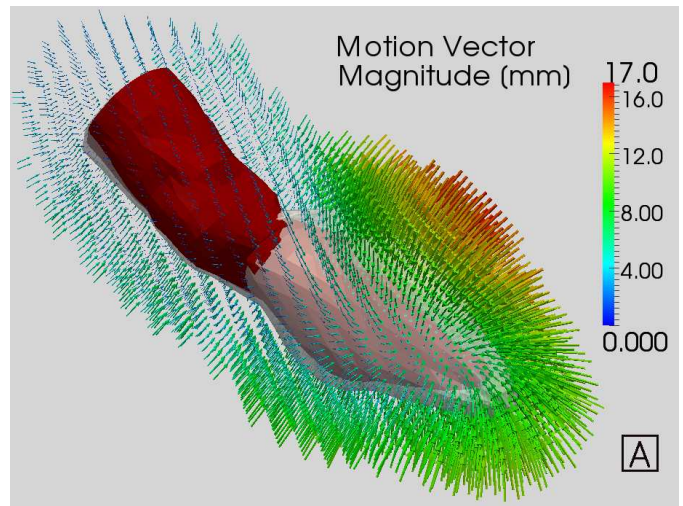


Fig. 1. Illustration of a dense MVF of the human data set computed with TPS between reference heart phase 70% and current phase 20%. Undersampled for illustration purposes.

TABLE I  
RESULTS FOR THE LEFT VENTRICLE.

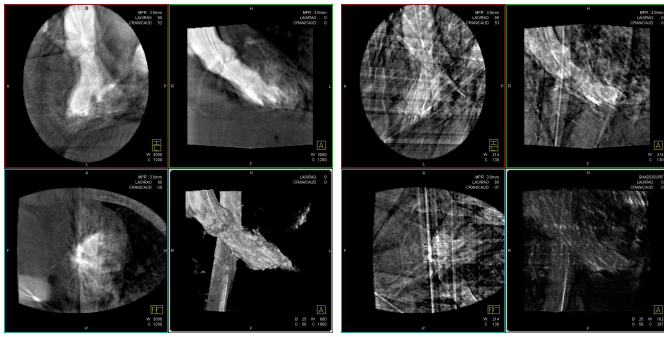
	Phantom		
	Dice [pixel]	$\epsilon$ [pixel]	$\epsilon$ [mm]
TPS	$0.95 \pm 0.03$	$3.26 \pm 0.37$	$2.02 \pm 0.23$
Shepard	$0.95 \pm 0.02$	$3.33 \pm 0.31$	$2.06 \pm 0.20$
Weighting Fct.	$0.95 \pm 0.02$	$3.33 \pm 0.27$	$2.06 \pm 0.17$
Simple Averaging	$0.94 \pm 0.02$	$3.64 \pm 0.33$	$2.26 \pm 0.20$
Standard	$0.94 \pm 0.03$	$4.66 \pm 1.91$	$2.89 \pm 1.18$
	Human		
	Dice [pixel]	$\epsilon$ [pixel]	$\epsilon$ [mm]
TPS	$0.93 \pm 0.01$	$9.15 \pm 1.22$	$1.65 \pm 0.22$
Shepard	$0.91 \pm 0.02$	$10.29 \pm 2.07$	$1.85 \pm 0.33$
Weighting Fct.	$0.91 \pm 0.02$	$10.92 \pm 3.02$	$1.97 \pm 0.54$
Simple Averaging	$0.91 \pm 0.03$	$11.74 \pm 2.81$	$2.11 \pm 0.51$
Standard	$0.88 \pm 0.03$	$17.60 \pm 10.0$	$3.17 \pm 1.80$

The standard deviation is also much smaller with the TPS compared to the standard reconstruction. The widely used Shepard's method and the weighting function provide slightly inferior results compared to the TPS. The Dice coefficient shows similar results between all interpolation methods as well as for the FDK reconstruction.

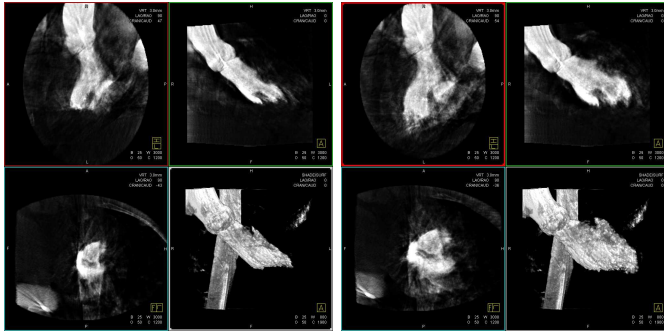
#### B. Clinical Data

In Table I the results for the human left ventricle are listed. The best motion compensated reconstruction is again performed with the TPS interpolation method. The contour deviation ( $\epsilon$ ) improved by  $\approx 9$  pixel which corresponds to 1.62 mm compared to the standard FDK. The patient had a healthy ejection fraction of  $\approx 75\%$ . The standard deviation is also much smaller with the TPS compared to the standard reconstruction. The widely used Shepard's method and the weighting function provides slightly inferior results compared to the TPS. The Dice coefficient again shows similar results between all interpolation methods as well as for the FDK reconstruction.

In Figure 2 the results of different reconstructions are illus-



(a) Standard FDK reconstruction. (b) Nearest-Neighbor ECG-gated reconstruction for 20% heart phase (5 views).



(c) Motion compensated reconstruction for 20% heart phase. (d) Motion compensated reconstruction for 70% heart phase.

Fig. 2. Reconstruction results of the human left ventricle with the TPS interpolation (W 3000, C 1200, Slice Thickness 3.0 mm). The ECG-gated reconstruction was windowed to be visually comparable.

trated. The standard reconstruction in Figure 2(a) exhibits blurring around the LV. In Figure 2(b) it can be observed that the ECG-gated reconstruction lacks LV structure. In comparison, the motion compensated reconstruction shows an expansion in diastole and contraction in systole of the LV, respectively (Fig.2(c),2(d)).

## V. CONCLUSION

In this paper, we investigated the influence of different motion interpolation methods for a left ventricle motion compensated tomographic reconstruction. The best quantitative results (Dice coefficient, mean contour deviation) of a phantom and human data set were achieved with the TPS interpolation approach. The Shepard's method and the weighting function might be a good compromise between computational efficiency and accuracy. In conclusion, motion compensated reconstruction improved the reconstruction results compared to a standard reconstruction.

## ACKNOWLEDGMENT

The authors would like to thank Drs. Patrick W. Serruys, Carl Schultz, Peter de Jaegere, and Robert van Geuns, Thorax Center, Erasmus MC, Rotterdam, The Netherlands for acquiring clinical data. Furthermore, the authors gratefully acknowledge funding of the NIH grant R01 HL087917 and of the Erlangen Graduate School in Advanced Optical Technologies (SAOT) by the German Research

Foundation (DFG) in the framework of the German excellence initiative.

**Disclaimer:** The concepts and information presented in this paper are based on research and are not commercially available.

## REFERENCES

- [1] M. Moriyama, Y. Sato, H. Naito, M. Hanayama, T. Ueguchi, T. Harada, F. Yoshimoto, and S. Tamura, "Reconstruction of time-varying 3-D left-ventricular shape from multiview x-ray cineangiocardiograms," *IEEE Trans. Med. Imag.*, vol. 21, no. 7, pp. 773–785, 2002.
- [2] L. Feldkamp, L. Davis, and J. Kress, "Practical cone-beam algorithm," *J. Opt. Soc. Am. A*, vol. 1, no. 6, pp. 612–619, 1984.
- [3] R. Medina, M. Garreau, H. Lebreton, and D. Jugo, "Three-dimensional reconstruction of the left ventricle from two angiographic views," in *IEEE EMBS*, October 1997, pp. 569–572.
- [4] B. Desjardins and E. Kazerooni, "Ecg-gated cardiac ct," *Am. J. Roentgenol.*, vol. 182, no. 4, pp. 993–1010, 2004.
- [5] C. Blondel, G. Malandain, R. Vaillant, and N. Ayache, "Reconstruction of coronary arteries from a single rotational x-ray projection sequence," *IEEE Trans. Med. Imag.*, vol. 25, no. 5, pp. 653–663, 2006.
- [6] E. Hansis, D. Schäfer, O. Dössel, and M. Grass, "Projection-based motion compensation for gated coronary artery reconstruction from rotational x-ray angiograms," *Phys. Med. Biol.*, vol. 53, no. 14, pp. 3807–3820, 2008.
- [7] C. Rohkohl, G. Lauritsch, L. Biller, M. Prümmer, J. Boese, and J. Hornegger, "Interventional 4D motion estimation and reconstruction of cardiac vasculature without motion periodicity assumption," *Medical Image Analysis*, vol. 14, no. 5, pp. 687–694, 2010.
- [8] G. Lauritsch, J. Boese, L. Wigström, H. Kemeth, and R. Fahrig, "Towards cardiac c-arm computed tomography," *IEEE Trans. Med. Imag.*, vol. 25, no. 7, pp. 922–934, 2006.
- [9] M. Prümmer, J. Hornegger, G. Lauritsch, E. Wigström, L. Girard-Hughes, and R. Fahrig, "Cardiac c-arm ct: A unified framework for motion estimation and dynamic ct," *IEEE Trans. Med. Imag.*, vol. 28, no. 11, pp. 1836–1849, 2009.
- [10] M. Chen, Y. Zheng, K. Müller, C. Rohkohl, G. Lauritsch, J. Boese, G. Funka-Lea, J. Hornegger, and D. Comaniciu, "Automatic extraction of 3D dynamic left ventricle model from 2D rotational angiocardiogram," in *MICCAI 2011*, September 2011, pp. 471–478.
- [11] D. Schäfer, J. Borgert, V. Rasche, and M. Grass, "Motion-compensated and gated cone beam filtered back-projection for 3-D rotational x-ray angiography," *IEEE Trans. Med. Imag.*, vol. 25, no. 7, pp. 898–906, 2006.
- [12] I. Amidror, "Scattered data interpolation methods for electronic imaging systems: a survey," *J. Electron. Imaging*, vol. 11, no. 2, pp. 157–176, 2002.
- [13] P. Forthmann, U. Stevendaal, M. Grass, and T. Köhler, "Vector field interpolation for cardiac motion compensated reconstruction," in *IEEE NSS-MIC*, October 2008, pp. 4157–4160.
- [14] F. Bookstein, "Principal warps: Thin-plate splines and the decomposition of deformations," *IEEE Trans. Pattern Anal. Mach. Intell.*, vol. 11, no. 6, pp. 567–585, 1989.
- [15] M. Davis, A. Khotanzad, D. Flamig, and S. Harms, "A physics-based coordinate transformation for 3-D image matching," *IEEE Trans. Med. Imag.*, vol. 16, no. 3, pp. 317–328, 1997.
- [16] D. Shepard, "A two-dimensional interpolation function for irregularly-spaced data," in *ACM 1968*, 1968, pp. 517–524.
- [17] A. Isola, C. Metz, M. Schaap, S. Klein, W. Niessen, and M. Grass, "Coronary segmentation based motion corrected cardiac ct reconstruction," in *IEEE NSS-MIC*, October 2010, pp. 2026–2029.
- [18] D. Suter and F. Chen, "Left ventricular motion reconstruction based on elastic vector splines," *IEEE Trans. Med. Imag.*, vol. 19, no. 4, pp. 295–305, 2000.
- [19] W. Segars, M. Mahesh, T. Beck, E. Frey, and B. Tsui, "Realistic ct simulation using the 4D xcat phantom," *Med. Phys.*, vol. 35, no. 8, pp. 3800–3808, 2008.
- [20] K. Zou, A. Warfield, A. Bharatha, C. Tempany, M. Kaus, S. Haker, W. Wells, F. Jolesz, and R. Kikinis, "Statistical validation of image segmentation quality based on a spatial overlap index: Scientific reports," *Acad. Radiol.*, vol. 11, no. 2, pp. 178–189, 2004.